# Enhanced High Voltage Performance of Chlorine/Bromine Co-Doped Lithium Nickel Manganese Cobalt Oxide

**Huali Zhu [1,2]**, **Qifeng Li [3]**, **Xiaolong Gong [3]**, **Kaifeng Cao [3]** and **Zhaoyong Chen [3,*]**

[1] School of Physics and Electronic Science, Changsha University of Science and Technology, Changsha 410114, China; juliezhu2005@126.com

[2] Department of Chemistry and Materials Science Program, University of New Hampshire, Durham, NH 03824, USA

[3] College of Materials Science and Engineering, Changsha University of Science and Technology, Changsha 410114, China; liqifeng26@163.com (Q.L.); L2AZ15874006546@163.com (X.G.); Browdervin@stu.csust.edu.cn (K.C.)

[*] Correspondence: chenzhaoyongcioc@126.com; Tel.: +86-137-8711-2902

**Abstract:** The chlorine (Cl) and bromine (Br) co-doped lithium nickel manganese cobalt oxide ($LiNi_{1/3}Co_{1/3}Mn_{1/3}O_2$) was successfully synthesized by the molten salt method. The synthesized $LiNi_{1/3}Co_{1/3}Mn_{1/3}O_2$ compound demonstrates spherical morphology, which is formed by aggregated spherical-like or polygon primary particles. Halogen substitution would contribute to the growth of the primary particles. The $LiNi_{1/3}Co_{1/3}Mn_{1/3}O_2$ compound has the typical hexagonal layered structure, and no impurity phase is detected. The surface oxidation state of the compound is improved after Cl and Br substitution. Moreover, the Cl and Br co-doped $LiNi_{1/3}Co_{1/3}Mn_{1/3}O_2$ compound exhibits both improved rate capacity and cycle stability at a high voltage (4.6 V) compared with the pristine $LiNi_{1/3}Co_{1/3}Mn_{1/3}O_2$. The initial discharge capacities of Cl and Br co-doped $LiNi_{1/3}Co_{1/3}Mn_{1/3}O_2$ are 208.9 mAh g$^{-1}$, 200.6 mAh g$^{-1}$, 188.2 mAh g$^{-1}$, 173.3 mAh g$^{-1}$, and 157.1 mAh g$^{-1}$ at the corresponding rates of 0.1C, 0.2C, 0.5C, 1C, and 3C respectively. The capacity retention at 1C after 50 cycles is increased from 81.1% to 93.2% by co-doping. The better contact between the electroactive particles of the electrode and the smaller resistance enhance the electric conductivity of the Cl and Br co-doped $LiNi_{1/3}Co_{1/3}Mn_{1/3}O_2$ cathode. The synthesized $LiNi_{1/3}Co_{1/3}Mn_{1/3}O_2$ is a promising cathode material for a high-power and large-capacity lithium-ion battery.

**Keywords:** lithium nickel manganese cobalt oxide; chlorine and bromine co-doping; high voltage; cathode material; lithium-ion battery

## 1. Introduction

The tremendous demand for a high-power and large-capacity lithium-ion battery is still ongoing, which is suitable for the energy storage systems of electric vehicles and power stations supplied by wind and solar energy [1–3]. Among the various components of a lithium-ion battery, the cathode material is a key factor in optimizing the overall performance of a battery. In recent years, $LiNi_{1/3}Co_{1/3}Mn_{1/3}O_2$ proposed by Ohzuku and Makimura [4] has been investigated extensively as a promising cathode material due to its higher performance and lower cost compared with commercial $LiCoO_2$. In the pristine $LiNi_{1/3}Co_{1/3}Mn_{1/3}O_2$ structure, the Co, Ni, and Mn exist in the oxidation states of +3, +2/+3 and +3/+4, respectively. The redox process at 2.5~4.4 V corresponds to the $Ni^{2+}/Ni^{4+}$ couple, and that at 4.4~4.6 V corresponds to the $Co^{3+}/Co^{4+}$ couple. Much attention has been given to the

improvements of its structural stability and electrochemical behavior below 4.5 V [5–9]. In our previous work, $LiNi_{1/3}Co_{1/3}Mn_{1/3}O_2$ cathode materials were synthesized by the molten salt method, and the electrochemical performance between 2.8–4.4 V was investigated [10,11]. Although the optimized $LiNi_{1/3}Co_{1/3}Mn_{1/3}O_2$ compounds exhibit an improved electrochemical performance, the cycling behavior at high voltage (especially above 4.4 V) should be further enhanced [12–14]. It was presumed that the mechanism of capacity fading for $LiNi_{1/3}Co_{1/3}Mn_{1/3}O_2$ at the high voltage was mainly attributed to the structure transformation and the gradual dissolution of Co and Mn [14,15]. It was also reported that the capacity fading of $LiNi_{1/3}Co_{1/3}Mn_{1/3}O_2$ in the potential region of 2.5–4.6 V was larger than that of 2.5–4.4 V because of the larger charge transfer resistance due to the low electric conductivity [16]. The research on the mechanism of capacity fading of $LiNi_{1/3}Co_{1/3}Mn_{1/3}O_2$ at the high voltage is still in progress. In order to suppress the structure transformation and the dissolution and improve the electrical conductivity of the compounds, the metal oxides were coated onto or substituted for $LiNi_{1/3}Co_{1/3}Mn_{1/3}O_2$, such as $Li_2O$-$B_2O_3$-$Li_2SO_4$, $ZrO_2$, $CeO_2$, ALD, $TiO_2$, $FePO_4$, and $Li_2MnO_3$ [17–23]. Meanwhile, several research groups have paid attention to the anion substitution for oxygen in order to improve the cyclic performances of the cathode material at the high voltage. The F substitution for oxygen in the $LiNi_{1/3}Co_{1/3}Mn_{1/3}O_2$ cathode material improved the thermal stability and the electrochemical property of $LiNi_{1/3}Co_{1/3}Mn_{1/3}O_2$ at 4.6 V [14,24]. The improved low voltage (4.3 V) performance of Cl-doped and Br-doped $LiNi_{1/3}Co_{1/3}Mn_{1/3}O_2$ was reported [25]. The enhanced lithium ion diffusions of F, Cl, and Br-substituted spinel $LiMn_2O_4$ were demonstrated in our previous works [26,27]. In brief, the substitution of halogen ions for the O anion has a significant influence on the physical and chemical performance of the cathode materials.

In this paper, the Cl and Br co-doped $LiNi_{1/3}Co_{1/3}Mn_{1/3}O_2$ was synthesized by the molten salt method. The morphological, structural, surface oxidation state, and high-voltage electrochemical properties of the Cl and Br co-doped $LiNi_{1/3}Co_{1/3}Mn_{1/3}O_2$ were compared with the pristine $LiNi_{1/3}Co_{1/3}Mn_{1/3}O_2$.

## 2. Materials and Methods

$LiNi_{1/3}Co_{1/3}Mn_{1/3}O_2$ compounds were synthesized by the molten salt method using $Ni_{1/3}Co_{1/3}Mn_{1/3}(OH)_2$ precursors (made in Kelong, Henan, China, Ni 21.63 wt%, Co 21.44 wt%, Mn 19.66 wt%), LiX (X = Cl, Br) and a stoichiometric amount of eutectic molten salts ($0.76LiOH·H_2O$-$0.24Li_2CO_3$). Cl and Br were used as the substitution for oxygen. The molar ratios of Cl and Br for the compound were both 0.05. According to the previous work [10], the stoichiometric $Ni_{1/3}Co_{1/3}Mn_{1/3}(OH)_2$, molten salts, and LiX were ground with a mortar and pestle. The mixture was put into the alumina crucible, heated up to 480 °C, and kept for 2 h; subsequently, it was heated to 850 °C with the heating rate of 3 °C min$^{-1}$ and kept for another 5 h again in the muffle furnace. Then, the synthesized $LiNi_{1/3}Co_{1/3}Mn_{1/3}O_2$ compounds (marked as the pristine LNCM and the Cl&Br co-doped LNCM here) were spontaneously cooled down to the ambient temperature. Finally, the compounds were washed with distilled water to remove the excess molten salts and dried at 100 °C.
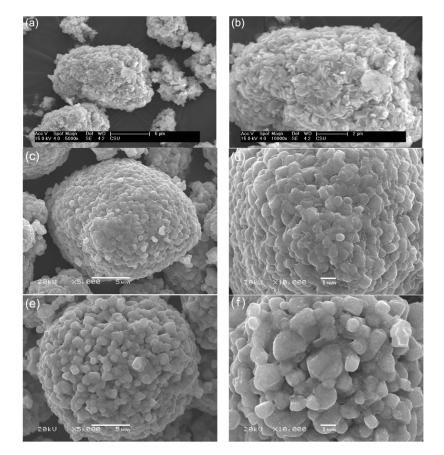
The morphology and energy dispersive spectroscopy (EDS) analysis of the synthesized compounds were observed with scanning electron microscopy (SEM, JSM5600LV, JEOL USA, Inc., 11 Dearborn Road, Peabody, MA 01960). The phase purity and crystal structure were characterized by X-ray diffractometry (XRD, D/max-2000, Rigaku, Tokyo, Japan) with Cu-Kα radiation (λ = 1.54056 Å) operating at 30 kV and 30 mA. The scan range was from 10° to 80°, and a step of 0.01° was used. The lattice parameters *a* and *c* were calculated after full profile fitting using the MDI Jade 5.0 software. The surface properties of the LNCM compounds were investigated by X-ray photoelectron spectroscopy (XPS, K-Alpha 1063, Thermo Fisher Scientific, 168 Third Avenue, Waltham, MA, USA 02451) using a monochromatic X-ray generated from Al Kα (1486.6 eV).

The positive electrode consisted of 85% as-prepared composites, 10% acetylene black and 5% polyvinylidene fluoride (PVDF) as a binder, and metal Al foil was used as a collector. Celgard 2400 was used as separator, which was soaked in 1.0 mol L$^{-1}$ $LiPF_6$/EC + DMC (EC:DMC = 1:1 in volume

ratio) electrolyte. Lithium metal foil was used as the counter electrode during the electrochemical measurements. All of the cells were assembled in an argon-filled glove box. The charge–discharge tests were carried out using a Land BT2001A automatic battery test system. The charge–discharge tests were completed in the voltage range of 2.5–4.6 V. AC impedance measurements were carried out with the scanning range of 1 mHz to 100 kHz using a CHI660B electrochemical workstation system (CH Instrument, Shanghai, China). All of the tests were performed at room temperature.
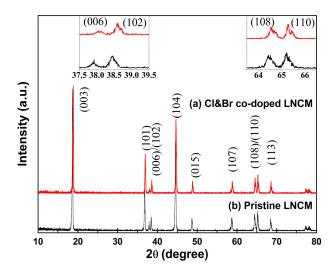
## 3. Results and Discussions

The SEM images of the precursor and the synthesized $LiNi_{1/3}Co_{1/3}Mn_{1/3}O_2$ compounds are illustrated in Figure 1. As can be observed from Figure 1a,b, the spherical $Ni_{1/3}Co_{1/3}Mn_{1/3}(OH)_2$ precursor compounds consist of flake-shaped primary particles, with an average diameter of ~10 μm. The pristine and halogen Cl and Br co-doped LNCM compounds keep the spherical morphology and consist of spherical-like or polygon primary particles, with an average diameter bigger than 10 μm, as shown in Figure 1c–f. The average primary particle diameter of the Cl and Br co-doped LNCM (~1.5 μm) is larger than that of the pristine LNCM (~1 μm). Cl and Br substitution would contribute to the growth of the primary particles of the $LiNi_{1/3}Co_{1/3}Mn_{1/3}O_2$ compound, which is consistent with the foregoing research on the fluorine-doped spinel $LiMn_2O_4$ [26]. With Cl and Br co-doping, the size of the primary particle becomes bigger, and the space between the primary particles increases, as shown in Figure 1f, which may allow the electrolyte solution to penetrate into the surface of these primary particles quickly.



**Figure 1.** SEM images of the $Ni_{1/3}Co_{1/3}Mn_{1/3}(OH)_2$ precursor and the synthesized $LiNi_{1/3}Co_{1/3}Mn_{1/3}O_2$ compounds: (**a,b**) $Ni_{1/3}Co_{1/3}Mn_{1/3}(OH)_2$ precursor; (**c,d**) Pristine LNCM; (**e,f**) Cl&Br co-doped LNCM.

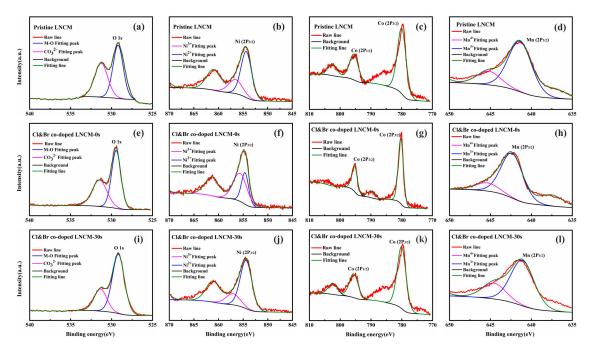The X-ray diffraction patterns of the synthesized $LiNi_{1/3}Co_{1/3}Mn_{1/3}O_2$ compounds are shown in Figure 2. The results reveal that the $LiNi_{1/3}Co_{1/3}Mn_{1/3}O_2$ compounds have the typical hexagonal layered structure of a-$NaFeO_2$ type with the space group *R-3m*. No obvious impurity phase is detected. In the typical XRD patterns of the $LiNi_{1/3}Co_{1/3}Mn_{1/3}O_2$ cathode material, the peak splits of (006)/(102) and (108)/(110) are known to be indicators of a layered structure [28]. The clear peak splits of (006)/(102) and (108)/(110) are observed from Figure 2, which indicate the highly ordered layered structure of the prepared $LiNi_{1/3}Co_{1/3}Mn_{1/3}O_2$ compounds. With Cl and Br co-doped, the positions of the (006)/(102) and (108)/(110) peaks move to higher angles, and the degrees of splitting increase. From Figure 2, it is shown that the Cl and Br co-doped sample shows a kind of reflection splitting that is most clearly visible for the (108) reflection, but also for the (110) and (102) reflections shown within the insets. Generally, this points to a multi-phase composition of the sample, i.e., probably two *R-3m* layered phases with slightly different lattice constants due to a different content of either Cl&Br or alternatively Li, which also has a strong influence on the lattice parameters. The integrated intensity ratio of the $(I_{006} + I_{102})/I_{101}$ and $I_{003}/I_{104}$ has been recognized as the criterion of the layered $LiNi_{1/3}Co_{1/3}Mn_{1/3}O_2$ crystal structure [29–31]. A value of $I_{003}/I_{104}$ less than 1.2 has been recognized as a criterion for the existence of undesirable cation mixing in the layered $LiNi_{1/3}Co_{1/3}Mn_{1/3}O_2$ compound. Furthermore, the intensity ratio of $(I_{006} + I_{102})/I_{101}$ is an indicator of the hexagonal ordering; the lower the value, the better the hexagonal ordering. In our experiments, the higher $I_{003}/I_{104}$ and the lower $(I_{006} + I_{102})/I_{101}$ values indicate a well-defined layered structure and less cation disordering, helping to exhibit better electrochemical performance. This result is proven in the following electrochemical measurements. It can be speculated that halogen ions doping enhanced the structural stability. Our results are accordance with those obtained for the chlorine doping [23].



**Figure 2.** XRD patterns of the synthesized $LiNi_{1/3}Co_{1/3}Mn_{1/3}O_2$ compounds: (**a**) Cl&Br co-doped LNCM; (**b**) Pristine LNCM.

The core-level XPS spectra of Ni 2p, Co 2p, Mn 2p, and O 1s for the synthesized $LiNi_{1/3}Co_{1/3}Mn_{1/3}O_2$ compounds are shown in Figure 3. All of the spectra were energy calibrated with the C 1s standard using the energy value of 284 eV, and then fitted using the Thermo Avantage software. It was reported that the Ni $2p_{3/2}$ binding energy observed at 854.0 eV was consistent with that of NiO [14], while the Ni $2p_{3/2}$ binding energy observed at 855.1 eV was aroused with the folding of $Ni(OH)_2$ and $Ni_2O_3$ [32]. As shown in Figure 3, the Ni $2p_{3/2}$ binding energy peak is observed at 854.5 eV. Therefore, the Ni cations in the pristine sample may consist of $Ni^{2+}$ and $Ni^{3+}$ oxidation states. The relative amounts of $Ni^{2+}$ and $Ni^{3+}$ are estimated to be 75.31% and 24.69% using the software. The Co $2p_{3/2}$ binding energy observed at 779.66 eV is consistent with that of $Co_2O_3$ [14]. The Co of the pristine LNCM is the $Co^{3+}$ oxidation state in a pristine LNCM compound. The Mn $2p_{3/2}$ binding energies of $Mn^{3+}/Mn^{4+}$ should be observed at 641.4/642.4 eV, according to reports in the
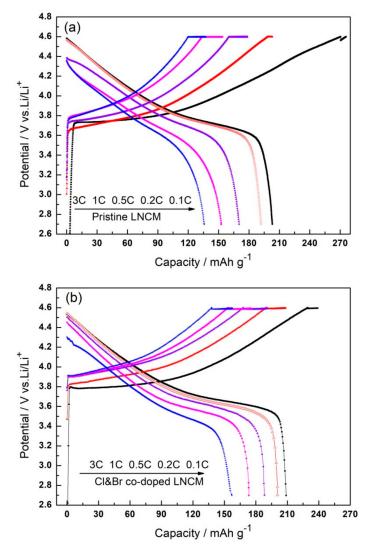
literature [14,33,34]. The Mn $2p_{3/2}$ XPS of the pristine LNCM centers at 641.7 eV, which indicates that the oxidation state of Mn of the pristine LNCM is a mixed oxidation state of $Mn^{3+}$ and $Mn^{4+}$. In the case of Cl and Br co-doped LNCM, the spectra of $Ni2p_{3/2}$, $Co2p_{3/2}$, and $Mn2p_{3/2}$ shift to higher binding energy, indicating that the valences of the transition metals increase. The relative amounts of $Ni^{2+}$ and $Ni^{3+}$ are estimated to 70.06% and 29.94%, respectively. The binding energy for $Mn2p_{3/2}$ of the Cl and Br co-doped LNCM is 642.24 eV, which agrees well with that of $Mn^{4+}$ reported in the literature [34]. After being ion-etched for 30 s, the Ni, Mn, and Co XPS core level spectra of the Cl and Br co-doped LNCM shift back to almost the same binding energy of the pristine LNCM. This indicates that the doping mainly affected the surface oxidation state of LNCM, and only happened to the surface near the regions of the material. This is probably because the synthesized $Ni_{1/3}Co_{1/3}Mn_{1/3}(OH)_2$ precursors were used to prepare the LNCM compound, and it is hard for Cl and Br to diffuse into the bulk material uniformly.



**Figure 3.** XPS spectra of (**a**) O 1s, (**b**) Ni $2p_{3/2}$, (**c**) Co 2 $p_{3/2}$, (**d**) Mn $2p_{3/2}$ for Pristine LNCM; (**e**) O 1s, (**f**) Ni $2p_{3/2}$, (**g**) Co $2p_{3/2}$, (**h**) Mn $2p_{3/2}$ for Cl&Br co-doped LNCM; (**i**) O 1s, (**j**) Ni $2p_{3/2}$, (**k**) Co $2p_{3/2}$, (**l**) Mn $2p_{3/2}$ for Cl&Br co-doped LNCM being ion-etched for 30 s.
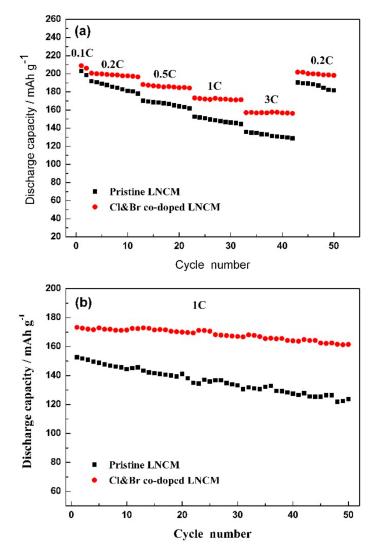
The initial charge/discharge capacities and the cyclic performances of the synthesized $LiNi_{1/3}Co_{1/3}Mn_{1/3}O_2$ compounds were evaluated at different rates in 2.5~4.6 V at room temperature. Figure 4 shows the initial charge/discharge curves of the synthesized $LiNi_{1/3}Co_{1/3}Mn_{1/3}O_2$ compounds at 0.1C, 0.2C, 0.5C, 1C, and 3C respectively. The pristine LNCM delivers discharge capacities of 203.1 mAh $g^{-1}$, 191.8 mAh $g^{-1}$, 170.2 mAh $g^{-1}$, 152.6 mAh $g^{-1}$, and 135.8 mAh $g^{-1}$, while the Cl and Br co-doped LNCM delivers 208.9 mAh $g^{-1}$, 200.6 mAh $g^{-1}$, 188.2 mAh $g^{-1}$, 173.3 mAh $g^{-1}$, and 157.1 mAh $g^{-1}$ at the corresponding rates of 0.1C, 0.2C, 0.5C, 1C, and 3C, respectively. The initial discharge capacities of Cl and Br co-doped LNCM are 5.8 mAh $g^{-1}$, 8.8 mAh $g^{-1}$, 18 mAh $g^{-1}$, 20.7 mAh $g^{-1}$, and 21.3 mAh $g^{-1}$ higher than the pristine one at the corresponding rates, respectively. It is indicated that the initial electrochemical capacity has been improved by Cl and Br co-doping. As shown in SEM analysis, the pores on the surface of co-doped LNCM can increase the contact area of the electrode/electrolyte, and also provide channels for the intercalation/deintercalation of lithium ions. More $Ni^{2+}$ exists in the pristine LNCM, which can cause more cation disordering, as shown in XPS analysis, and a larger $R_{(sei+ct)}$ value, which is discussed in

the following electrochemical impedance spectra measurement (EIS) analysis, may lead to a lower initial coulomb efficiency of pristine LNCM than the Cl and Br co-doped LNCM.
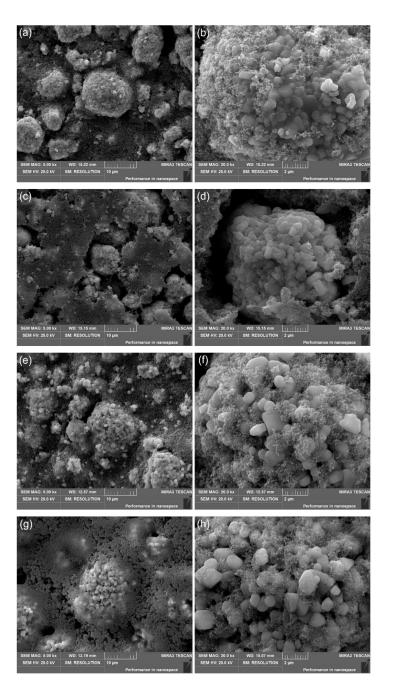


**Figure 4.** Initial charge and discharge capacities of the synthesized $LiNi_{1/3}Co_{1/3}Mn_{1/3}O_2$ compounds at 0.1~3C: (**a**) Pristine LNCM; (**b**) Cl&Br co-doped LNCM.

The cycle performances of the synthesized $LiNi_{1/3}Co_{1/3}Mn_{1/3}O_2$ compounds at different rates are shown in Figure 5. It demonstrates that the Cl and Br co-doped LNCM has an excellent cycle stability, and it can restore to the initial capacity of 0.1C after two cycles at 0.1C, 10 cycles at 0.2C, 0.5C, 1C, 3C, and then back to 0.2C, respectively, while the capacities of the pristine LNCM decrease rapidly. The cyclic curves of the pristine LNCM and the Cl and Br co-doped LNCM at 1C for 50 cycles show that the initial and 50th discharge capacities, and the capacity retention of the Cl and Br co-doped LNCM are 173.3 mAh g$^{-1}$, 161.5 mAh g$^{-1}$, and 93.2% respectively, which are obviously higher than the pristine LNCM (152.6 mAh g$^{-1}$, 123.7 mAh g$^{-1}$, and 81.1% for comparison). We presume that the good cycle performance of the Cl and Br co-doped LNCM compounds benefits from the enhanced structure stability after doping and the $Mn^{4+}$ in the surface layer of the $LiNi_{1/3}Co_{1/3}Mn_{1/3}O_2$ compounds, which can avoid the dissolution and the John-Teller effect of $Mn^{3+}$. Also, the observed differences in rate capability should rather be attributed to the different morphology, which is a side effect of doping, or rather to the surface doping on an atomic level, probably by the change of electronic structure or diffusion.

**Figure 5.** Rate capabilities (**a**) and cycling performance (**b**) of the synthesized $LiNi_{1/3}Co_{1/3}Mn_{1/3}O_2$ compounds.

After cycling for 100 cycles, the cells were disassembled and washed with dimethylcarbonate in the argon-filled glove box to completely remove the residual lithium salts. The SEM images of the synthesized $LiNi_{1/3}Co_{1/3}Mn_{1/3}O_2$ electrodes are shown in Figure 6. It can be seen that the surface morphology of the pristine $LiNi_{1/3}Co_{1/3}Mn_{1/3}O_2$ electrode changes a lot. The obvious cracks appear between the $LiNi_{1/3}Co_{1/3}Mn_{1/3}O_2$ composites and acetylene black particles, which result in inferior contact between the electroactive $LiNi_{1/3}Co_{1/3}Mn_{1/3}O_2$ particles during the charge–discharge process. As to the Cl and Br co-doped LNCM electrode, the surface morphology almost doesn't change, and the acetylene black still covers the $LiNi_{1/3}Co_{1/3}Mn_{1/3}O_2$ particles completely, which may keep the effective conductive behavior during cycling. It may be the contribution of the space between primary particles, as shown in Figure 1, that stably adhere the acetylene black onto the surface of the $LiNi_{1/3}Co_{1/3}Mn_{1/3}O_2$ particles. Chemical composition (wt%) of the electrodes determined by energy dispersive spectroscopy (EDS) with the particles in Figure 6b,d,f,g are listed in Table 1. The molar ratio of Ni:Co:Mn has a small variation after being cycled. It indicates that Mn dissolution is depressed by halogen doping, which would keep the structure stability.
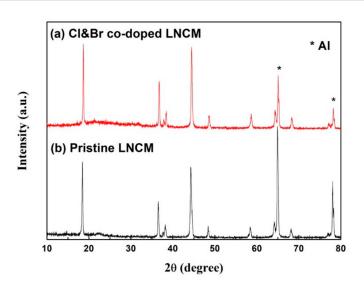
**Figure 6.** SEM images of the synthesized $LiNi_{1/3}Co_{1/3}Mn_{1/3}O_2$ electrodes after cycling (100 cycles): (**a**,**b**) Pristine LNCM before cycling; (**c**,**d**) Pristine LNCM after cycling; (**e**,**f**) Cl&Br co-doped LNCM before cycling; (**g**,**h**) Cl&Br co-doped LNCM after cycling.

XRD patterns of the synthesized $LiNi_{1/3}Co_{1/3}Mn_{1/3}O_2$ electrodes after 100 cycles at 1C are shown in Figure 7. Except for the peaks at 65° and 77°, which represent the metal Al foil, there are no impurity peaks. The $(I_{006} + I_{102})/I_{101}$ values increase, and the $I_{003}/I_{104}$ values decrease after cycling. These results demonstrate that the two samples keep the layered structure, but the cation ordering in the layered hexagonal structure was changed in the pristine LNCM compound. The Cl and Br co-doped LNCM keeps a better crystallinity than the pristine one, as the densities of diffraction peaks are higher than the latter.
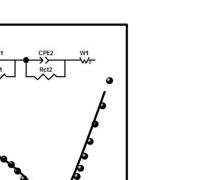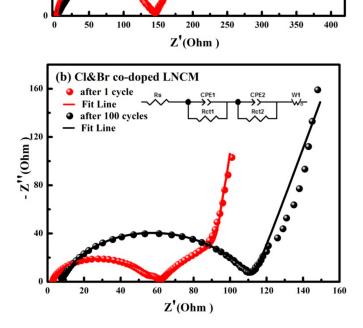
**Table 1.** Chemical composition (wt%) of the electrodes determined by energy dispersive spectroscopy (EDS) with the particles in Figure 6b,d,f,g.

| Sample | Ni (wt%) | Co (wt%) | Mn (wt%) | Molar Ratio of Ni:Co:Mn |
|---|---|---|---|---|
| fresh pristine LNCM | 20.04 | 19.40 | 18.39 | 0.340:0.327:0.333 |
| cycled pristine LNCM | 22.75 | 22.40 | 19.60 | 0.345:0.338:0.317 |
| fresh Cl&Br co-doped LNCM | 22.11 | 21.72 | 20.07 | 0.339:0.332:0.329 |
| cycled Cl&Br co-doped LNCM | 21.56 | 20.52 | 19.16 | 0.345:0.327:0.328 |



**Figure 7.** XRD patterns of the synthesized $LiNi_{1/3}Co_{1/3}Mn_{1/3}O_2$ electrodes after 100 cycles: (**a**) Cl&Br co-doped LNCM; (**b**) Pristine LNCM.

Electrochemical impedance spectra measurements were carried out for the pristine LNCM and Cl and Br co-doped LNCM electrodes after the first and 100th cycle. The obtained results are shown in Figure 8. The impedance plots show a high-frequency intercept at the Z′ axis, a broad depressed semicircle, and a straight line in the low-frequency region. The high-frequency intercept is due to the ohmic resistance ($R_s$). The depressed semicircle is related to the formation of a surface layer on the active material and the intercalation/deintercalation of lithium ions into/from the electrodes. An equivalent circuit used to fit the spectra is shown in the inset of Figure 8a [35]. The spectra are fitted using a combination of surface film and charge transfer resistance, $R_{(sei+ct)}$, and the corresponding constant phase element (CPE). The $R_{(sei+ct)}$ values of the pristine LNCM and Cl and Br co-doped LNCM after the first/100th cycle are calculated as 142 $\Omega$/308 $\Omega$ and 59 $\Omega$/104 $\Omega$, respectively. Cl and Br co-doped LNCM has a smaller $R_{(sei+ct)}$ value than the pristine one. The reduced $R_{(sei+ct)}$ value favored the electrochemical reaction upon lithium ion intercalation/deintercalation, which implied the enhanced the cyclic stability. These results are in accordance with the electrochemical charge–discharge test.

**Figure 8.** Electrochemical impedance spectra of the synthesized LiNi$_{1/3}$Co$_{1/3}$Mn$_{1/3}$O$_2$ electrodes after different cycles: (**a**) Pristine LNCM; (**b**) Cl&Br co-doped LNCM.

## 4. Conclusions

A Cl and Br co-doped LiNi$_{1/3}$Co$_{1/3}$Mn$_{1/3}$O$_2$ compound was synthesized by the molten salt method. It was characterized by scanning electron microscopy (SEM), energy dispersive spectroscopy (EDS), X-ray diffraction (XRD), X-ray photoelectron spectroscopy (XPS), galvanostatic charge–discharge measurements and electrochemical impedance spectra measurement (EIS). SEM results show that the pristine and halogen co-doped LiNi$_{1/3}$Co$_{1/3}$Mn$_{1/3}$O$_2$ compounds keep the spherical morphology consisting with spherical-like or polygon primary particles. Cl and Br substitution would contribute to the growth of the primary particles. The XRD results demonstrate that the LiNi$_{1/3}$Co$_{1/3}$Mn$_{1/3}$O$_2$ compound has the typical hexagonal layered structure, and no impurity phase is detected. XPS results indicated that the surface oxidation state of the compound is improved with Cl and Br substitution. The Cl and Br co-doped LiNi$_{1/3}$Co$_{1/3}$Mn$_{1/3}$O$_2$ compound exhibits both an improved rate capacity and cycle stability at a high voltage (4.6 V) compared with the pristine LiNi$_{1/3}$Co$_{1/3}$Mn$_{1/3}$O$_2$. The initial discharge capacities of Cl and Br co-doped LiNi$_{1/3}$Co$_{1/3}$Mn$_{1/3}$O$_2$ are 208.9 mAh g$^{-1}$, 200.6 mAh g$^{-1}$, 188.2 mAh g$^{-1}$, 173.3 mAh g$^{-1}$, and 157.1 mAh g$^{-1}$ at the corresponding rates of 0.1C, 0.2C, 0.5C, 1C, and 3C, respectively. The capacity retention after 50 cycles at 1C is increased from 81.1% to 93.2% after doping. The better contact between the electroactive particles of the electrode and the smaller resistance would enhance the electric conductivity of the Cl and Br co-doped LiNi$_{1/3}$Co$_{1/3}$Mn$_{1/3}$O$_2$ cathode.

## References

1. Goodenough, J.B.; Kim, Y. Challenges for rechargeable batteries. *J. Power Sources* **2011**, *196*, 6688–6694. [CrossRef]

2. Chen, Z.; Qin, Y.; Amine, K.; Sun, Y.-K. Role of surface coating on cathode materials for lithium-ion batteries. *J. Mater. Chem.* **2010**, *20*, 7606–7612. [CrossRef]

3. Li, H.; Zhou, H. Enhancing the performances of Li-ion batteries by carbon-coating: Present and future. *Chem. Commun.* **2012**, *48*, 1201–1217. [CrossRef] [PubMed]

4. Ohzuku, T.; Makimura, Y. Layered Lithium insertion material of $LiNi_{1/2}Mn_{1/2}O_2$: A possible alternative to $LiCoO_2$ for advanced lithium-ion batteries. *Chem. Lett.* **2001**, *30*, 744–745. [CrossRef]

5. Roberts, M.; Owen, J. High-throughput method to study the effect of precursors and temperature, applied to the synthesis of $LiNi_{1/3}Co_{1/3}Mn_{1/3}O_2$ for lithium batteries. *ACS Comb. Sci.* **2011**, *13*, 126–134. [CrossRef] [PubMed]

6. Yang, C.; Zhang, X.; Huang, M.; Huang, J.; Fang, Z. Preparation and Rate Capability of Carbon Coated $LiNi_{1/3}Co_{1/3}Mn_{1/3}O_2$ as Cathode Material in Lithium Ion Batteries. *ACS Appl. Mater. Interfaces* **2017**, *9*, 12408–12415. [CrossRef] [PubMed]

7. Gao, P.; Li, Y.; Liu, H.; Pinto, J.; Jiang, X.; Yang, G. Improved high rate capacity and lithium diffusion ability of $LiNi_{1/3}Co_{1/3}Mn_{1/3}O_2$ with ordered crystal structure. *J. Electrochem. Soc.* **2012**, *159*, A506–A513. [CrossRef]

8. Jiang, K.-C.; Xin, S.; Lee, J.-S.; Kim, J.; Xiao, X.-L.; Guo, Y.-G. Improved kinetics of $LiNi_{1/3}Mn_{1/3}Co_{1/3}O_2$ cathode material through reduced graphene oxide networks. *Phys. Chem. Chem. Phys.* **2012**, *14*, 2934–2939. [CrossRef] [PubMed]

9. Zhang, Y.; Jia, D.; Tang, Y.; Huang, Y.; Pang, W.; Guo, Z.; Zhou, Z. In situ chelating synthesis of hierarchical $LiNi_{1/3}Co_{1/3}Mn_{1/3}O_2$ polyhedron assemblies with ultralong cycle life for Li-ion batteries. *Small* **2018**, *14*, 1704354. [CrossRef] [PubMed]

10. Zhu, H.; Li, J.; Chen, Z.; Li, Q.; Xie, T.; Li, L.; Lai, Y. Molten salt synthesis and electrochemical properties of $LiNi_{1/3}Co_{1/3}Mn_{1/3}O_2$ cathode materials. *Synth. Met.* **2014**, *187*, 123–129. [CrossRef]

11. Chen, Z.Y.; Xie, T.; Li, L.J.; Xu, M.; Zhu, H.L.; Wang, W.H. Characterization of Na substituted $LiNi_{1/3}Co_{1/3}Mn_{1/3}O_2$ cathode materials for lithium ion battery. *Ionics* **2014**, *20*, 629–634. [CrossRef]

12. Shaju, K.M.; Rao, G.V.S.; Chowdari, B.V.R. Performance of layered $Li(Ni_{1/3}Co_{1/3}Mn_{1/3})O_2$ as cathode for Li-ion batteries. *Electrochim. Acta* **2002**, *48*, 145–151. [CrossRef]

13. Periasamy, P.; Kalaiselvi, N.; Kim, H.S. High voltage and high capacity characteristics of $LiNi_{1/3}Co_{1/3}Mn_{1/3}O_2$ cathode for lithium battery applications. *Int. J. Electrochem. Sci.* **2007**, *2*, 689–699.

14. Kim, G.-H.; Kim, J.-H.; Myung, S.-T.; Yoon, C.S.; Sun, Y.-K. Improvement of high-voltage cycling behavior of surface-modified $Li[Ni_{1/3}Co_{1/3}Mn_{1/3}]O_2$ cathodes by fluorine substitution for li-ion batteries. *J. Electrochem. Soc.* **2005**, *152*, A1707–A1713. [CrossRef]

15. Zeng, Y.W. Investigation of $LiNi_{1/3}Co_{1/3}Mn_{1/3}O_2$ cathode particles after 300 discharge/charge cycling in a lithium-ion battery by analytical TEM. *J. Power Sources* **2008**, *183*, 316–324. [CrossRef]

16. Li, X.; Wei, Y.J.; Ehrenberg, H.; Du, F.; Wang, C.Z.; Chen, G. Characterizations on the structural and electrochemical properties of $LiNi_{1/3}Mn_{1/3}Co_{1/3}O_2$ prepared by a wet-chemical process. *Solid State Ionics* **2008**, *178*, 1969–1974. [CrossRef]

17. Lv, D.; Wang, L.; Hu, P.; Sun, Z.; Chen, Z.; Zhang, Q.; Cheng, W.; Ren, W.; Bian, L.; Xu, J.; et al. $Li_2O$-$B_2O_3$-$Li_2SO_4$ modified $LiNi_{1/3}Co_{1/3}Mn_{1/3}O_2$ cathode material for enhanced electrochemical performance. *Electrochim. Acta* **2017**, *247*, 803–811. [CrossRef]

18. Li, X.; Peng, H.; Wang, M.-S.; Zhao, X.; Huang, P.-X.; Yang, W.; Xu, J.; Wang, Z.-Q.; Qu, M.-Z.; Yu, Z.-L. Enhanced electrochemical performance of Zr-modified layered $LiNi_{1/3}Co_{1/3}Mn_{1/3}O_2$ cathode material for lithium-ion batteries. *ChemElectroChem* **2015**, *3*, 130–137. [CrossRef]

19. Wu, F.; Wang, M.; Su, Y.; Bao, L.; Chen, S. Surface of $LiCo_{1/3}Ni_{1/3}Mn_{1/3}O_2$ modified by $CeO_2$-coating. *Electrochim. Acta* **2009**, *54*, 6803–6807. [CrossRef]

20. Riley, L.A.; Atta, S.V.; Cavanagh, A.S.; Yan, Y.; George, S.M.; Liu, P.; Dillon, A.C.; Lee, S.-H. Electrochemical effects of ALD surface modification on combustion synthesized $LiNi_{1/3}Mn_{1/3}Co_{1/3}O_2$ as a layered-cathode material. *J. Power Sources* **2011**, *196*, 3317–3324. [CrossRef]

21. Li, J.; Fan, M.; He, X.; Zhao, R.; Jiang, C.; Wan, C. $TiO_2$ coating of $LiNi_{1/3}Co_{1/3}Mn_{1/3}O_2$ cathode materials for Li-ion batteries. *Ionics* **2006**, *12*, 215–218. [CrossRef]

22. Liu, X.; Li, H.; Yoo, E.; Ishida, M.; Zhou, H. Fabrication of $FePO_4$ layer coated $LiNi_{1/3}Co_{1/3}Mn_{1/3}O_2$: Towards high-performance cathode materials for lithium ion batteries. *Electrochim. Acta* **2012**, *83*, 253–258. [CrossRef]

23. Son, M.Y.; Hong, Y.J.; Choi, S.H.; Kang, Y.C. Effects of ratios of $Li_2MnO_3$ and $Li(Ni_{1/3}Mn_{1/3}Co_{1/3})O_2$ phases on the properties of composite cathode powders in spray pyrolysis. *Electrochim. Acta* **2013**, *103*, 110–118. [CrossRef]

24. Li, D.; Sasaki, Y.; Kobayakawa, K.; Noguchi, H.; Sato, Y. Preparation, morphology and electrochemical characteristics of $LiNi_{1/3}Mn_{1/3}Co_{1/3}O_2$ with LiF addition. *Electrochim. Acta* **2006**, *52*, 643–648. [CrossRef]

25. Chen, Y.; Jiao, Q.; Wang, L.; Hu, Y.; Sun, N.; Shen, Y.; Wang, Y. Synthesis and characterization of $Li_{1.05}Co_{1/3}Ni_{1/3}Mn_{1/3}O_{1.95}X_{0.05}$ (X = Cl, Br) cathode materials for lithium-ion battery. *C. R. Chim.* **2013**, *16*, 845–849. [CrossRef]

26. Chen, Z.Y.; Zhu, H.L.; Hu, G.R.; Xiao, J.; Peng, Z.D.; Liu, Y.X. Electrochemical performances and structure characteristic of $LiMn_2O_{4-x}Y_x$(Y = F, Cl, Br) compounds. *Trans. Nonferrous Met. Soc. China* **2004**, *14*, 1151–1155.

27. Chen, Z.-Y.; Gao, L.Z.; Liu, X.Q.; Yu, Z.L. Properties and structure of spinel Li-Mn-O-F compounds for cathode materials of secondary lithium-ion battery. *Chin. J. Chem.* **2011**, *19*, 347–351. [CrossRef]

28. Gao, Y.; Yakovleva, M.V.; Ebner, W.B. Novel $LiNi_{1-x}Ti_{x/2}Mg_{x/2}O_2$ compounds as cathode materials for safer lithium-ion batteries. *Electrochem. Solid-State Lett.* **1998**, *1*, 117–119. [CrossRef]

29. Zhang, X.; Jiang, W.J.; Mauger, A.; Lu, Q.; Gendrond, F.; Julien, C.M. Minimization of the cation mixing in $Li_{1+x}(NMC)_{1-x}O_2$ as cathode material. *J. Power Sources* **2010**, *195*, 1292–1301. [CrossRef]

30. Reimers, J.N.; Rossen, E.; Jones, C.D.; Dahn, J.R. Structure and electrochemistry of $Li_xFe_yNi_{1-y}O_2$. *Solid State Ionics* **1993**, *61*, 335–344. [CrossRef]

31. Ohzuku, T.; Ueda, A.; Nagayama, M. Electrochemistry and structural chemistry of $LiNiO_2$ (R3m) for 4 volt secondary lithium cells. *J. Electrochem. Soc.* **1993**, *140*, 1862–1870. [CrossRef]

32. Oswald, S.; Brückner, W. XPS depth profile analysis of non-stoichiometric NiO films. *Surf. Interface Anal.* **2004**, *36*, 17–22. [CrossRef]

33. Kageyama, M.; Li, D.; Kobayakawa, K.; Sato, Y.; Lee, Y.-S. Structural and electrochemical properties of $LiNi_{1/3}Mn_{1/3}Co_{1/3}O_{2-x}F_x$ prepared by solid state reaction. *J. Power Sources* **2006**, *157*, 494–500. [CrossRef]

34. Iwanowski, R.J.; Heinonen, M.H.; Janik, E. X-ray photoelectron spectra of zinc-blende MnTe. *Chem. Phys. Lett.* **2004**, *387*, 110–115. [CrossRef]

35. Zhu, H.L.; Xie, T.; Chen, Z.Y.; Li, L.J.; Xu, M.; Wang, W.H.; Lai, Y.Q.; Li, J. The impact of vanadium substitution on the structure and electrochemical performance of $LiNi_{0.5}Co_{0.2}Mn_{0.3}O_2$. *Electrochim. Acta* **2014**, *135*, 77–85. [CrossRef]